Very Stable Ribonucleotide Substrate Radical Relevant for Class I Ribonucleotide Reductase

Fahmi Himo and Per E. M. Siegbahn*

Department of Physics, Stockholm University, Box 6730, S-113 85 Stockholm, Sweden

Received: February 29, 2000; In Final Form: May 4, 2000

In recent experimental studies on the E441Q mutant of ribonucleotide reductase, a new substrate radical was discovered on the minute time scale. This radical is kinetically coupled to a cysteine-based radical appearing on the 10 s time scale. In the present study, density functional calculations have been performed to investigate the nature of these radicals. The most interesting result is that a very stable substrate radical was found, which lies outside the normal substrate pathway. This radical is so stable that its creation has to be avoided by the enzyme, or the substrate reactions would be slowed by several orders of magnitude. It is suggested that the enzyme accomplishes this task by considerably straining the mobility of the Cys225 residue. A previously suggested reaction mechanism is modified to take these recent findings into account. The modification does not significantly change the energetics of the model reactions.

I. Introduction

Ribonucleotide reductase (RNR) catalyzes the transformation shown in Figure 1, in which a ribonucleotide is converted into a 2′ deoxyribonucleotide.[1] Four classes of RNR, each one with a different metallo-cofactor, have been characterized.[2−4] The class I RNR enzymes consist of two homodimeric proteins, R1 and R2,[5] where an iron dimer is present in R2. In a reaction between the diferrous form of this dimer and an oxygen molecule, a radical is created at Tyr122 close to the iron dimer. This tyrosyl radical is connected to the substrate site in the R1 protein, about 35 Å away, through a chain of hydrogen-bonded residues.[3] In a step preceding the substrate reactions, it is assumed that the radical is transferred from Tyr122 to Cys439 at the substrate site,[3] in a process that is likely to at least partially be hydrogen atom transfer between amino acid residues in the hydrogen-bonded path.[6,7] Using the Cys439 radical as a catalyst, the substrate ribonucleotide is converted into the deoxyribonucleotide, in a process where a water molecule is lost and a disulfide bond is formed between two essential cysteines, Cys225 and Cys462.[2] After this transformation is finished the radical returns back to Tyr122 in R2 through the hydrogen-bonded path.

The X-ray structures of both the R1 and R2 proteins of RNR have been determined, the one of R2 by Nordlund et al.[8] and the one of R1 by Uhlin et al.[9] More recently, the structure of R1 including a substrate was also determined, by Eriksson et al.[10] The substrate region of this structure is shown in Figure 2. As seen in this figure, the ribonucleotide is bound by hydrogen bonds to its hydroxyl oxygen atoms. These hydrogen bonds are formed to Glu441 at the C3′ oxygen and to Asn437 at the C2′ oxygen. The beginning of the hydrogen-bonded path from Cys439 to Tyr122 is marked in the figure, with hydrogen bonds to Tyr730 and Tyr731.

In recent years there has been substantial progress in the understanding at a molecular level of the different steps of the substrate reactions of RNR. On the basis of isotopic labeling, kinetic, spectroscopic, and site-directed mutagenesis experiments, and also theoretical calculations, a reaction mechanism has been suggested by Stubbe et al.[2,11,12] As new results have become available, the mechanism has been revised several times and the most recent version is shown in Figure 3. In the first step a hydrogen atom from C3′ of the ribonucleotide substrate is abstracted by the Cys439 radical. In the second step, a proton is abstracted by the C2′ hydroxyl of the substrate from a cysteine, leading to formation of a water molecule. On the basis of theoretical studies,[14] an initial carboxylate anion of Glu441 is suggested to simultaneously abstract a proton from the C3′ hydroxyl group. This leaves the substrate as a neutral radical species and the cysteine as an anion after step 2. Alternatively,

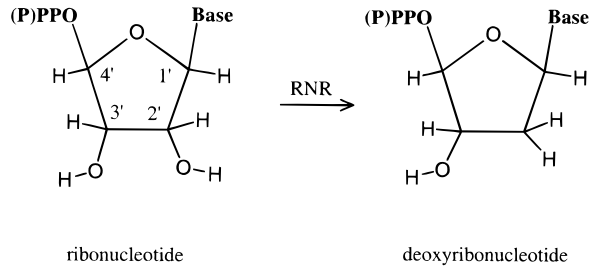

Figure 1. Transformation catalyzed by RNR.

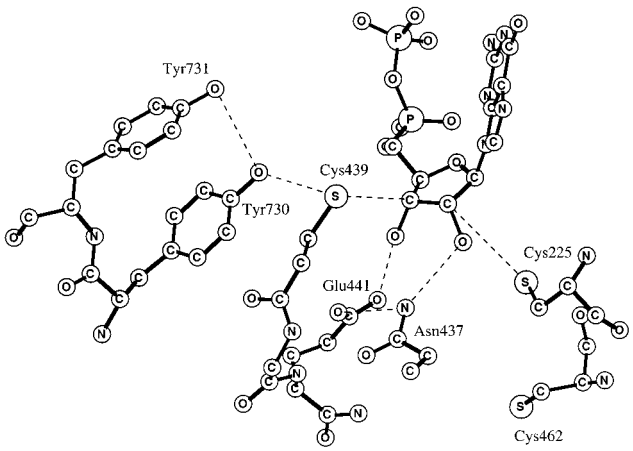

Figure 2. X-ray structure of the substrate region of the R1 subunit of *Escherichia coli* RNR.

10.1021/jp000752f CCC: $19.00
Published on Web 07/18/2000

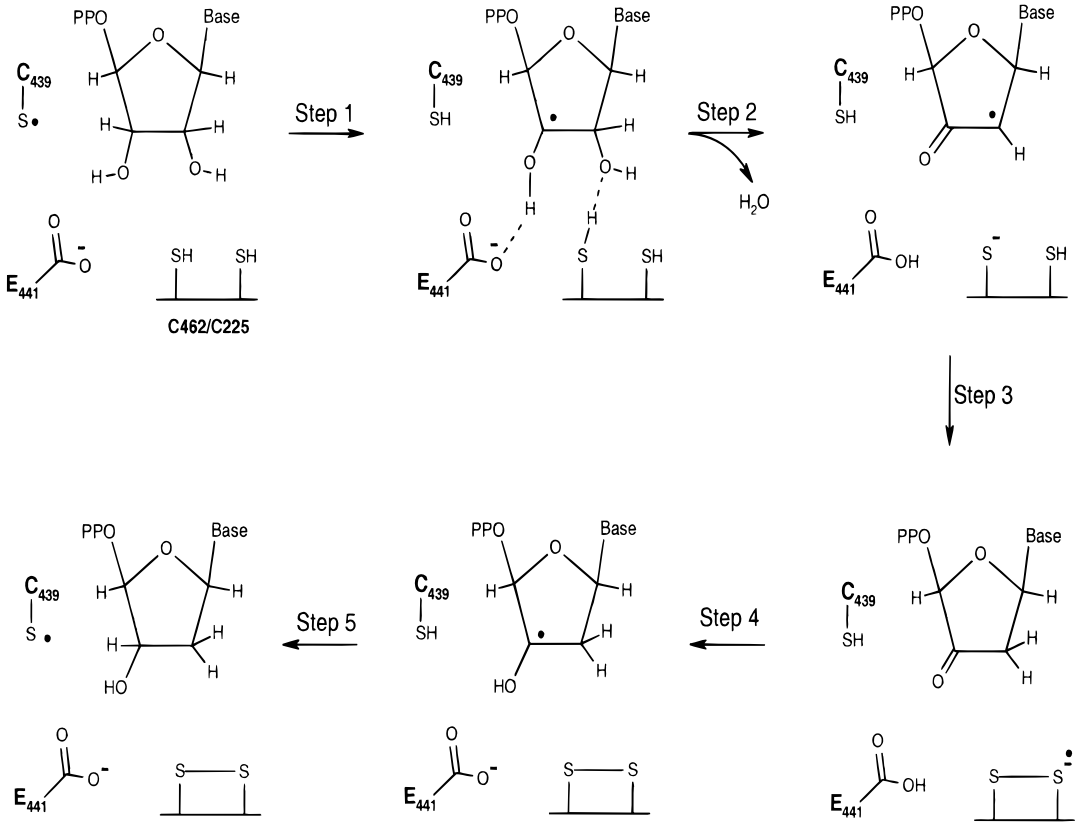

Figure 3. Experimentally suggested reaction mechanism for class I RNR.

mechanisms involving either a radical cation or radical anion have been invoked for this step on the basis of model systems.[15,16] In the third step, a hydrogen atom is abstracted by C2′ of the substrate from a cysteine, and the two cysteines (Cys225 and Cys462) form a disulfide anion. In the fourth step, the substrate abstracts an electron from the disulfide anion and a proton from Glu441 to form a hydroxyl at C3′. Finally, the C3′ radical can in the fifth step reabstract a hydrogen atom from Cys439 to complete the formation of the deoxyribonucleotide product.

The substrate reaction mechanism of RNR has also been studied theoretically by B3LYP density functional theory (DFT), leading to the suggested reaction sequence shown in Figure 4.[13] In step 1, a hydrogen atom is abstracted by Cys439 from C3′, exactly as in the experimentally suggested scheme. This abstraction is assisted by the presence of the Glu441 and Asn437 residues, which initiate the transfer of a hydrogen from the C3′−OH group to the C2′−OH. The completion of this transfer, leading to formation of a water molecule, occurs in the second step. This abstraction of the C2′−OH group was thus suggested to occur by a different mechanism than the one assumed in Figure 3, where a cysteine residue was proposed to be involved. On the other hand, the mechanism suggested for this step is very similar to the one proposed by Lenz and Giese on the basis of the chemistry of model compounds;[17] see also recent model work by Robins et al.[18] At the end of step 2, an oxaallylic radical is thus formed. In step 3 a hydrogen atom was suggested to be abstracted by C2′ from Cys225 leading to a stable species with a keto group, which is the resting state for the remaining steps of the cycle. To find a mechanism with a reasonable barrier for step 4 turned out to be very difficult. The mechanism with the lowest barrier found is one where the Cys225 group attacks the C3′ center of the ribose ring. This was suggested to occur by a simultaneous formation of a C−S and an O−H bond at the C3′ keto group. A cyclic transition state was proposed, including apart from Cys225 also Glu441 and a water molecule in the ring, and Asn437 outside the ring. In the fifth step, the disulfide bond between Cys225 and Cys462 was suggested to be formed assisted by the presence of Glu441 and Asn437. In the final sixth step, the deoxyribonucleotide should be formed in essentially the reverse of the first step exactly as proposed also in Figure 3.

Recent mutation experiments have shed new light on the substrate mechanism of RNR and represent the background for the reinvestigation of the mechanism undertaken in the present study. In these studies,[19−21] the active site glutamic acid Glu441 was replaced by a glutamine. In the theoretical scheme in Figure 4, Glu441 has an important role in step 2, where the water molecule is formed, by assisting in a proton transfer from the C3′ to C2′ hydroxyl groups. An even more important role is implied in the rate-limiting step 4, where a cyclic transition state involving Glu441 is suggested for the protonation of the keto group. Glu441 is also proposed to have important roles at similar stages of the experimentally suggested scheme in Figure 3. The mutation experiments show that the substrate reactions are interrupted at some stage, thus confirming the essential role of Glu441.

By means of rapid freeze quench EPR spectroscopy, Persson et al. detected two new transient, kinetically coupled radicals.[19] The first radical appears on the 10 s time scale and was shown to be cysteine-based, using a [β-^{2}H] cysteine-labeled enzyme.[20] Persson et al. suggested this radical to be the Cys439 thiyl radical. However, the g-values observed ($g_{av} = 2.01$) were not consistent with this assignment. Repeating the experiments at higher field (140 GHz), Lawrence et al. obtained g-tensor components ($g_1 = 2.023$, $g_2 = 2.015$, $g_3 = 2.002$) very similar to those of the disulfide radical anion,[21] which accordingly was proposed to be the source of the first radical. The second

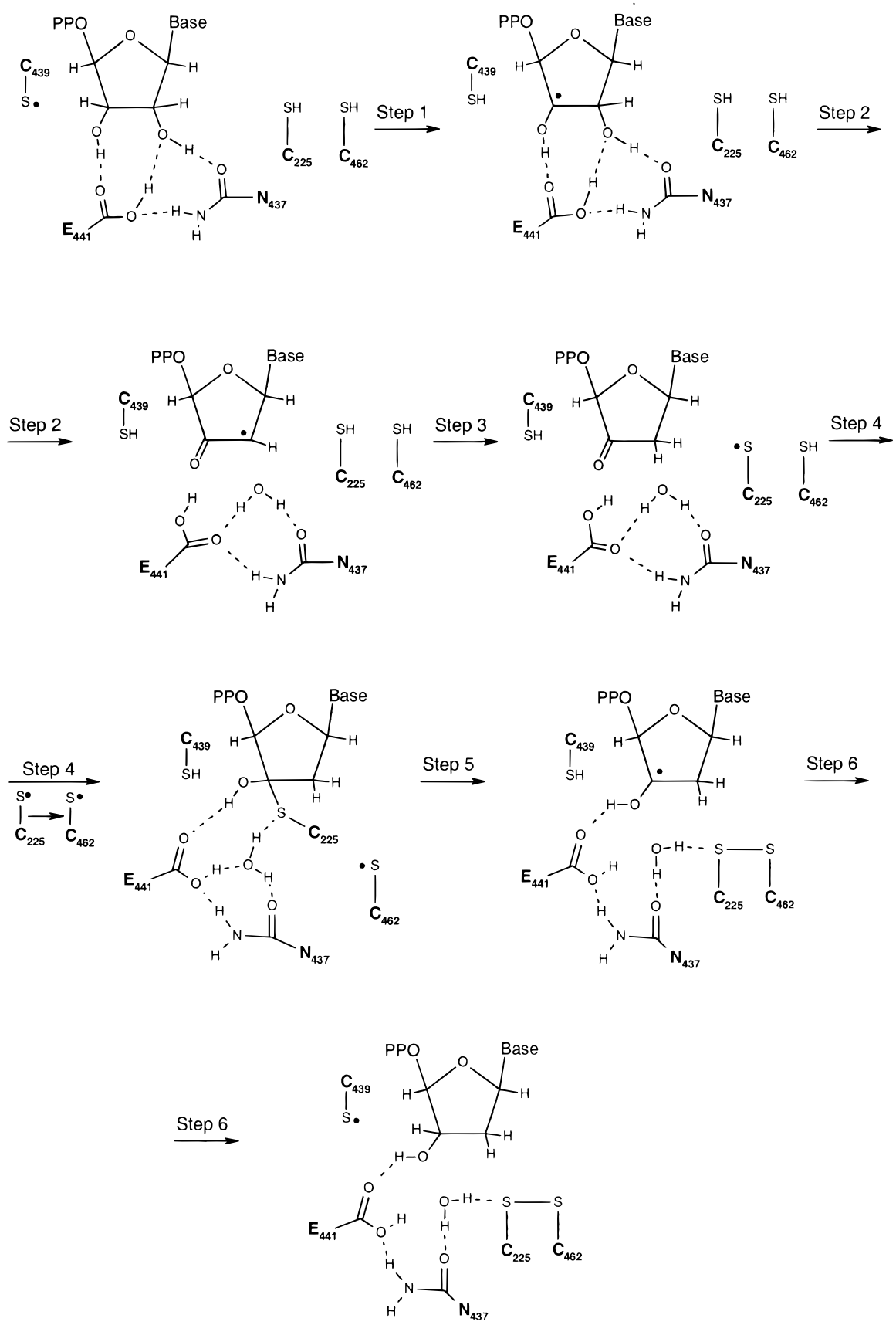

Figure 4. Theoretically suggested reaction mechanism for class I RNR.

transient radical was observed on the minute time scale. Using uniformly ^{13}C-labeled substrate, Persson et al. demonstrated that this radical is substrate-derived and was then assigned to be the 3′ radical created in the first step by hydrogen atom transfer to the Cys439 radical. From the high-field *g*-values, Lawrence et al. proved, however, that the radical cannot be the 3′ radical and suggested instead the 4′ radical, which is not on the normal substrate reduction pathway (see Figures 3 and 4).

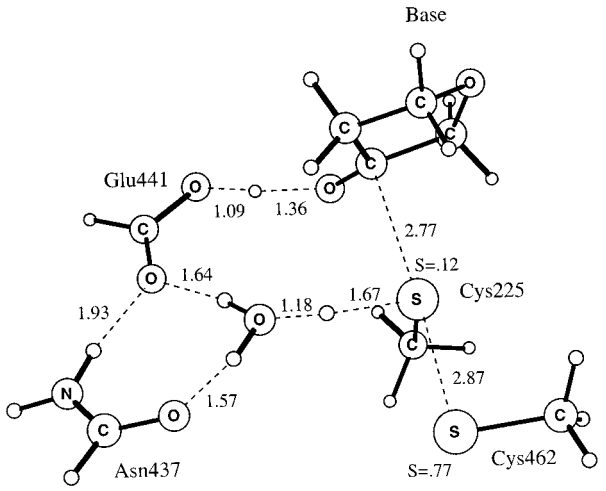

Figure 5. Transition state for protonation of the keto group of the substrate, including also Cys462.

Assuming the assignment of the disulfide radical anion is correct, which appears very likely, this means that the scheme in Figure 4 has to be somewhat modified, since the Cys462 radical is just a spectator in step 4. In the present paper, the effect of binding this radical to Cys225 is reinvestigated. It was investigated already in the previous study, but only for the smaller models. Also, different substrate radicals are studied for a possible identification of the radical observed at the minute time scale. As it turned out, these investigations, described in detail below, show that the C4′ radical is extremely stable, much more stable than was anticipated, which has significant implications for the substrate mechanism of RNR. However, only very small energetic effects were found for the models used to study the reaction mechanism in Figure 4.

II. Computational Details

The model calculations for the RNR reaction mechanism were made in two steps. First, an optimization of the geometry was performed using the B3LYP method[22] with double-ζ (d95) basis sets for first row atoms. For sulfur a larger triple-ζ basis was used with an added d-function (6-311G(d)). All degrees of freedom were optimized, and the transition states obtained were confirmed to have only one imaginary frequency of the Hessian. The use of small basis sets for this step is quite adequate since reaction energies have been found to be very insensitive to the accuracy of the geometries.[23] In the second step the B3LYP energy was evaluated for the optimized geometry using very large (6-311+G(2d,2p)) basis sets, which include diffuse functions and two sets of polarization functions on each atom. However, for the largest models only one set was used. All values reported include zero-point effects, evaluated at the same level as used for the geometries. Again, for the largest models a lower level was used with scaled (0.9) Hartree−Fock frequencies. Dielectric effects using the self-consistent reaction field (SCRF) method[24] were also evaluated. A dielectric constant of 4 was used, but since the effects are generally found to be quite small, the results are not sensitive to this precise choice. For the same reason, the geometries were determined without dielectric effects present, which is an excellent approximation for the present type of systems.[25] All calculations were made using the GAUSSIAN-94 program.[26] The spin distributions reported were obtained from a standard Mulliken population analysis using the d95 basis set. Finally, to test the accuracy of the B3LYP method for the present systems, a few calculations were done at a higher level for some of the substrate radicals. The method used for these tests was the G2MS method.[27]

III. Results and Discussion

With the background of the new experimental information available from the E441Q mutant,[19−21] two different issues are addressed in the present study. The first issue concerns the finding of a disulfide radical anion at the 10 s time scale. In particular, the possibility is investigated for forming the disulfide bond already in the step where the keto group of the substrate is protonated (step 4 in Figure 4). In the previous reaction sequence, the disulfide bond was suggested to be formed only at step 5. This investigation is reported in subsection a below. The second issue addressed is the structure of the substrate radical appearing at the minute time scale for the mutant. Different possible radicals are compared, and this investigation is reported in subsection b below.

a. The Formation of the Disulfide Bond. In the previous study,[13] a large number of different attempts were made to obtain a reasonable barrier for the protonation of the keto group in step 4. One of the first attempts was to protonate the keto group simultaneously as the disulfide bond is formed (see Figure 6 of ref 13). However, the calculated barrier was 24.5 kcal/mol, which is too high. In comparison, the lowest barrier obtained finally for the best model tried was only 12.4 kcal/mol. In this model, the radical cysteine is surprisingly just a spectator, and a cyclic transition state is formed including Glu441 and a critical water molecule in the ring and with Asn437 connected outside the ring; see Figure 4. The product of this reaction step is a substrate, which besides the protonated keto group also has Cys225 connected to C3′ via a C−S bond. This mechanism has the problem that it requires a flexible positioning of Cys225. It needs to reach both C2′ for deprotonation and C3′ for forming the C−S bond. From the recent X-ray structure including the substrate,[10] it is not clear that this is actually possible. This problem was noted in the previous study, and to test an alternative, where the C−S bond never needs to be formed, a model was set up including both cysteines and Glu441. The water molecule and Asn437 were left out. This model would in principle allow the protonation of the keto group without the formation of the C−S bond by instead forming a disulfide bond. Rather surprisingly, the barrier using this model was found to be 27.3 kcal/mol, which is much too high to be consistent with experiments. Before the results of the present model calculations are discussed, some results for the isolated disulfide anion and the neutral disulfide will be mentioned. First, a neutral disulfide, modeled by CH_3S-SCH_3, has a calculated S−S bond length of 2.1 Å and an S−S bond strength of 54 kcal/mol. In comparison, the disulfide anion $CH_3S-SCH_3^-$ radical has an S−S bond length as long as 2.9 Å and a much weaker S−S bond strength of 23 kcal/mol. Most of the bonding in this anion is due to a delocalization of the charge and is characteristic of a gas-phase situation. For the present type of enzyme models, it has generally been found that the best representation of the energetics is obtained if the model is kept neutral. Therefore, a sulfur of the disulfide is protonated, making it a neutral (CH_3)-$HS-SCH_3$ radical. This has a rather limited effect on the S−S bond, increasing it to 3.2 Å, but decreases the S−S bond strength all the way down to 0.8 kcal/mol. This bond strength is so small that it is questionable if this could be considered a chemical bond. However, despite the weak interaction the spin is somewhat delocalized with 0.85 and 0.15 on the sulfurs. This delocalization may explain how EPR can clearly distinguish between this disulfide radical as compared to a single cysteinyl radical,[21] despite the weak interaction.

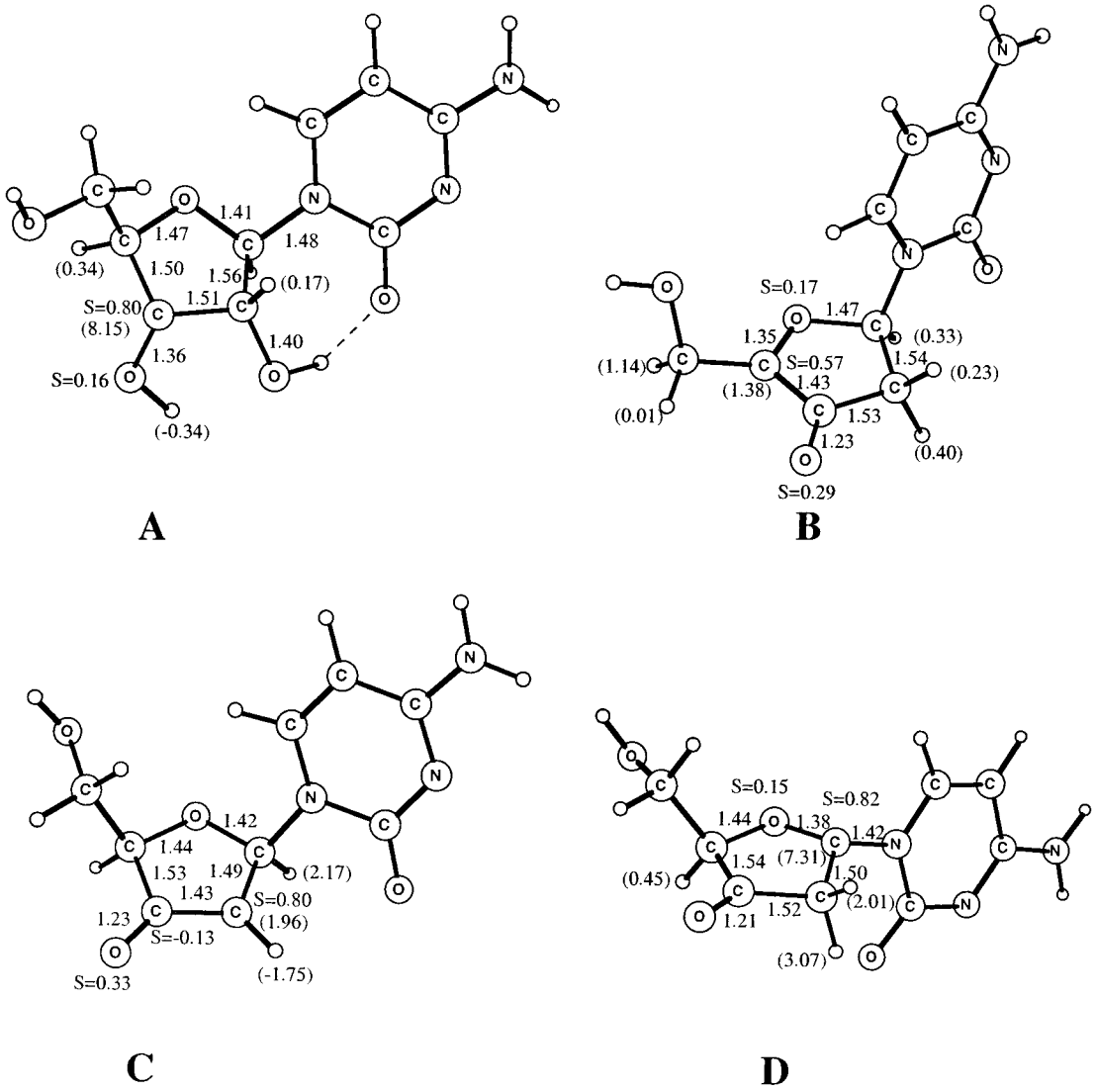

Figure 6. Structures and spin populations for the different substrate radicals studied in the present work. In parentheses, isotropic ^{1}H and ^{13}C hyperfine coupling constants are given in mT.

TABLE 1: C−H Bond Dissociation Energies (kcal/mol) for Different Carbon Centers of the Substrates Using Different Models for the Phosphate Group at C4′ and for the base at C1′[a]

phosphate	base	C4′	C2′	C1′
H	H	76.0	+10.9	+13.9
CH_2OH	H	73.2	+12.6	+15.8
CH_2OH	NH_2	71.2	+14.4	+18.0
H	cytosine	78.3	+9.0	+10.7
CH_2OH	cytosine	74.0	+12.9	+13.7

[a] The C−H bond strengths for C1′ and C2′ are given relative to the one for C4′.

In light of the recent experimental finding of the disulfide anion in the E441Q mutant, the transition state for step 4 was reinvestigated using the largest model used in the previous study and adding the radical cysteinyl (Cys462). This led to the transition state structure shown in Figure 5 for step 4. The calculated binding energy for the added Cys462 radical to the rest of the structure is only 1.1 kcal/mol, even though the S−S bond distance of 2.87 Å is the same as for a free disulfide anion. For the reactant the binding energy is actually slightly larger with 1.3 kcal/mol. At the transition state the spin has decreased on the sulfurs from 0.15 and 0.85 for the reactants to 0.12 and 0.77, and some spin is thus delocalized on the rest of the structure. The combined energetic effects lead to a total effect on the barrier from the added Cys462 radical of +0.2 kcal/mol.

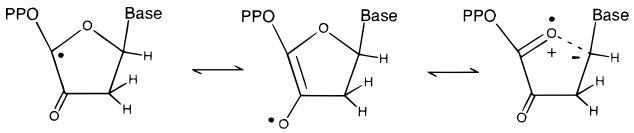

I II III

Figure 7. Resonance structures for the 4′ radical.

If it were only for the effect of 0.2 kcal/mol on the barrier height, the Cys462 radical could as well have been left out of the model calculations. However, there is one significant difference in the transition state structure of Figure 5 as compared to the one of the previous study. This difference concerns the distance between Cys225 and the C3′ center, which has increased from 2.4 to 2.8 Å. A distance of 2.8 Å is so long that it is more clear than before that the interaction between these centers is very weak at this point. One important consequence of this result is that the reaction can go directly to the neutral disulfide from the transition state, rather than first going to the C−S adduct. Another consequence is that the C−S

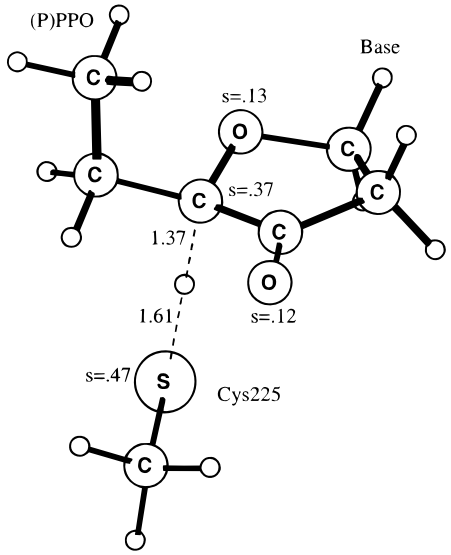

Figure 8. Transition state for hydrogen abstraction from C4′ of the substrate.

bond can be increased even further at the transition state without significantly increasing the barrier height. Taken together, the new transition state structure in Figure 5 implies that the large flexibility of Cys225 required previously is not needed anymore. However, at this stage it is not clear that the enzyme gains anything by preventing the C−S bond to be formed, but from the results of the next subsection it will be clear that it is actually mechanistically very important for the enzyme to hold Cys225 at a substantial distance away from the C4′ center, and thereby also away from the C3′ center.

b. The Structure of the Substrate Radical for the E441Q Mutant. In the recent mutation experiments described above, Persson et al. assigned the substrate radical to the 3′ radical occurring in the first step of the catalytic cycle.[19,20] Considering that the cysteine-based radical discussed above is not the Cys439 thiyl radical,[21] this assignment becomes questionable. In order analyze this issue further, calculations were performed on the 3′ radical. It turns out that the spin is highly localized to the C3′ carbon (0.80), resulting in a very high ^{13}C hyperfine coupling of over 8 mT on that center. Given that the peak-to-trough value in the detected ^{13}C spectrum is less than 3 mT,

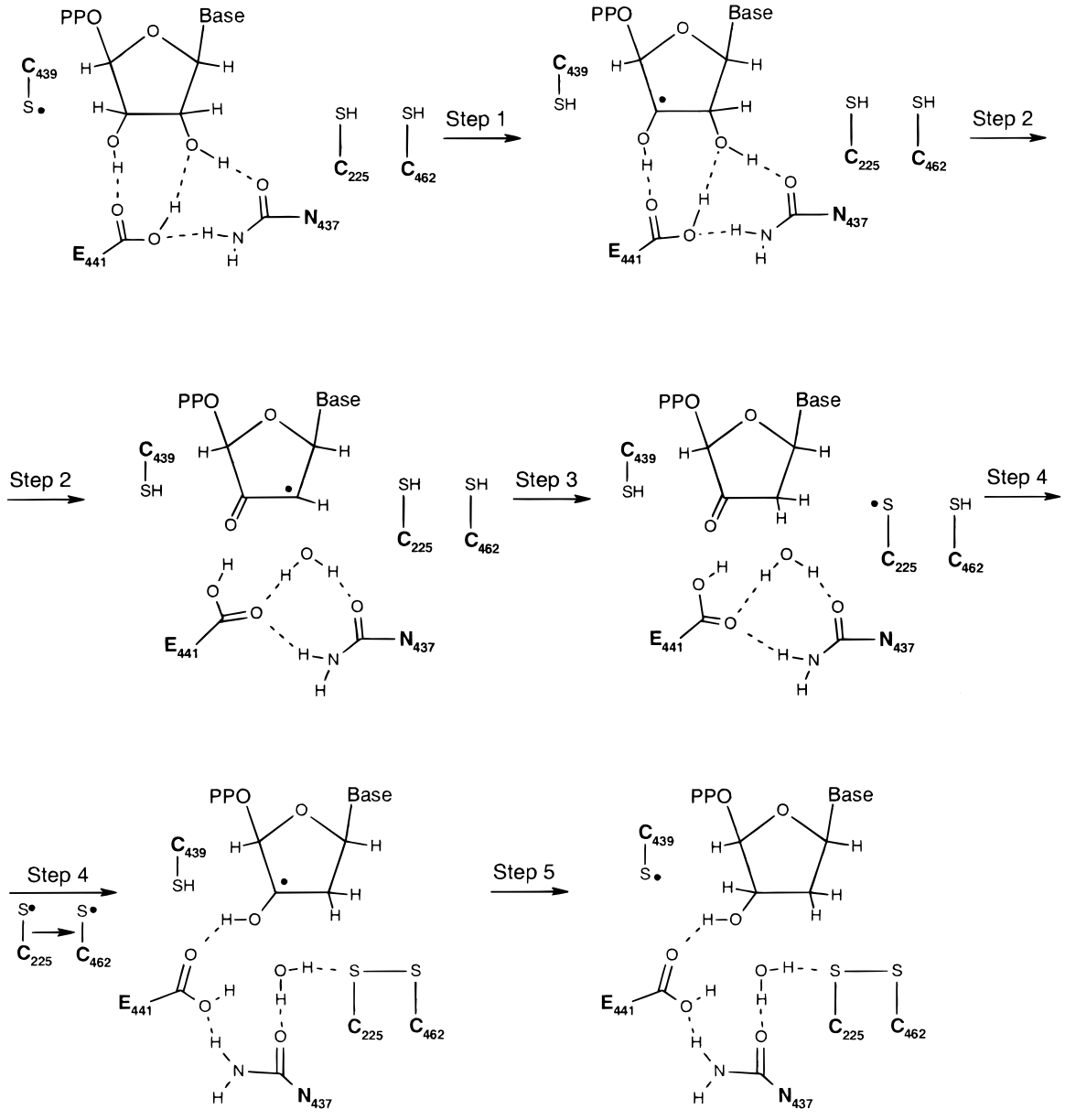

Figure 9. Modified theoretical reaction mechanism for class I RNR.

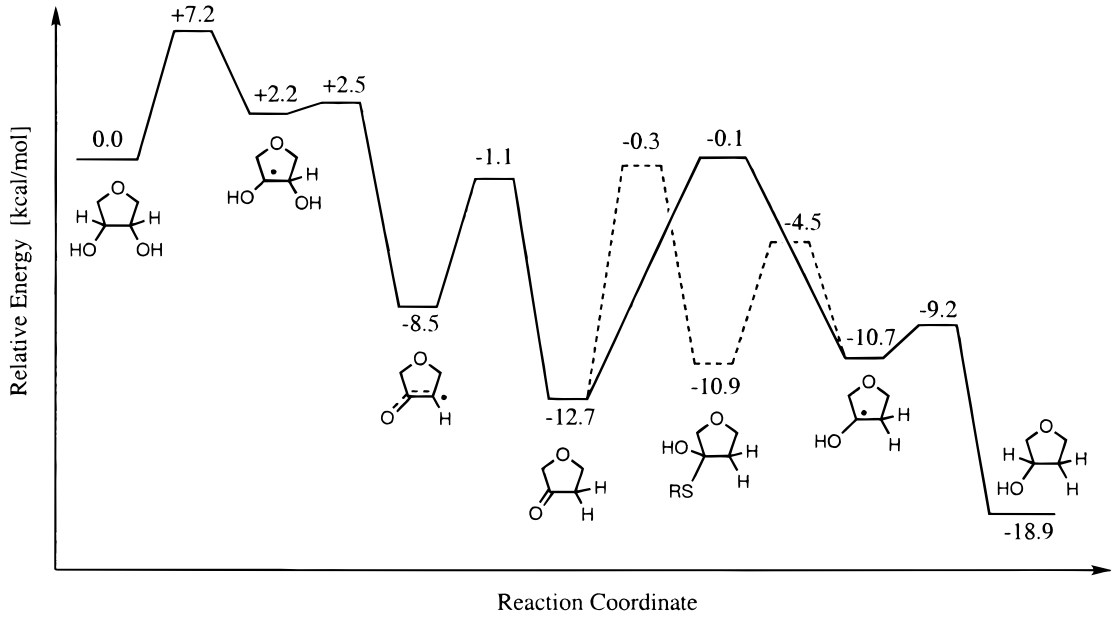

Figure 10. Energy diagram for the old (dashed) and the modified (solid) reaction mechanisms of class I RNR.

the calculations unambiguously rule out the 3′ radical as the 10 s transient radical. This is in full agreement with the conclusions of Lawrence et al. who instead suggested the substrate radical to be the 4′ ketyl radical (the 2′ ketyl radical is the one occurring after step 2 in the normal route). To test this suggestion, calculations were also performed for the 4′, 2′, and 1′ ketyl radicals for different models. The structures are shown in Figure 6 (structures B−D), and the energetic results are given in Table 1, where the energies of the 1′ and 2′ radicals are given relative to the 4′ radical. In the largest model, the base at 1′ is taken to be cytosine, and the phosphate ligand at 4′ is modeled by CH_2-OH. In the smaller models, the base was modeled by NH_2 or a hydrogen atom, and the phosphate ligand by a hydrogen atom. As apparent from the table, the 4′ radical is a very stable species. For the largest model, this radical is as much as 13.7 and 12.9 kcal/mol more stable than the 1′ and 2′ radicals, respectively.

By studying the bond distances, and the spin and charge distributions, the very high stability of the 4′ radical could be explained by the resonance forms displayed in Figure 7. Structures **I** and **II** are identical to the corresponding resonance forms present in the 2′ radical. What makes the 4′ radical much more stable than the 2′ radical is the ionic resonance **III**. Evidence for this resonance is seen particularly on the considerable amount of spin located on the ring oxygen (0.17), and also on the asymmetric bonding of this oxygen to the carbons. The O−C4′ bond is clearly shorter than in the parent molecule (1.35 vs 1.47 Å) and the O−C1′ bond longer (1.47 vs 1.41 Å). A similar ionic resonance is present in the 1′ radical, but here the resonance of type **II** does not exist, explaining why the 1′ radical is 13.7 kcal/mol less stable than the 4′ radical.

Since the high relative stability of the 4′ radical is somewhat surprising, a more advanced method was also used to calculate the energy differences for the smallest model. This method is the G2-MS method,[27] which extrapolates the CCSD(T) energy for a limited basis to a large basis using MP2. The G2-MS energies confirm the B3LYP values in Table 1. The relative stability using G2-MS for the 4′ radical is 12.3 kcal/mol compared to 1′ and 10.5 kcal/mol compared to 2′, which differ from the B3LYP values by only 1.6 and 0.4 kcal/mol, respectively.

The very high stability of the 4′ radical means that the formation of this radical must be prevented by the enzyme; otherwise, the activity would essentially stop. This can be realized by a simple comparison of stabilities. Since the reactant for the reaction leading to the transition state shown in Figure 5 is more stable than the C2′ radical by only 4.2 kcal/mol, it means that it is less stable by 12.9 − 4.2 = 8.7 kcal/mol than the C4′ radical. In turn, this means that the barrier for this reaction would be increased by 8.7 to 21.3 kcal/mol if the reaction was allowed to proceed to the C4′ radical. This would significantly slow the substrate reactions by 6 orders of magnitude.

The only possibility to prevent the formation of the stable C4′ radical is to have a high barrier for its formation. Using a simple model for hydrogen abstraction from C4′, as shown in Figure 8, a barrier of only 2 kcal/mol is found. The conclusion is that the formation of the C4′ radical instead has to be prevented by strain in the enzyme, holding Cys225 away from C4′. This strain has to be considerable and can be estimated in the following way. Assuming that the substrate radical observed for the E441Q mutant actually is the C4′ radical, the time scale for its formation of 3 min indicates that the barrier height for its formation using transition state theory is about 20 kcal/mol. Since the intrinsic barrier for the formation of the C4′ radical given by the model shown in Figure 8 is only 2 kcal/mol, the strain energy preventing Cys225 to reach C4′ should be 20 − 2 = 18 kcal/mol. Even if this estimate should be overestimated by a few kcal/mol, it is still quite considerable.

A few additional comments can be given on the energies in Table 1. Assuming the largest model is the best one, it can first be noted that it is actually better to model the base by a hydrogen atom than by NH_2. The NH_2 substituent gives rise to resonances not present in the actual base. Modeling the phosphate ligand is less sensitive and is slightly better using CH_2OH than a hydrogen atom. However, the modeling of both groups by hydrogen atoms does very well with rather small errors on the order of 1−2 kcal/mol for both absolute bond strengths and relative stabilities of the radicals, thus supporting the use of this model in the previous study.[13]

IV. Conclusions

The main result of the present study is that the C4′ keto radical of the substrate is extremely stable. In the best model, it is 13 kcal/mol more stable than the C2′ radical, which is on the normal substrate pathway (see step 2 in Figure 4). Since the C2′ radical is only 4.2 kcal/mol less stable than the keto group that is the resting state for the rate-limiting step 4, the formation of the C4′ radical must be avoided by the enzyme. If it were to form it would slow the substrate reactions by several orders of magnitude. Since the C4′ radical could easily form by hydrogen abstraction using a cysteinyl radical after step 3 with almost no barrier, Cys225 must be held away from C4′ as much as possible. The enzyme therefore constrains the motion of Cys225 considerably. On the basis of the measured reaction rate for creating the substrate radical in the mutation experiment, and assuming the C4′ radical is created, the strain energy for reaching the C4′ position is estimated to be larger than 15 kcal/mol. Owing to this strain, Cys225 cannot form the C−S bond to C3′ either, as previously suggested on the basis of calculations (see step 4 in Figure 4), since C3′ is too close to C4′. Instead, in the protonation chemistry in step 4, Cys225 will have to directly form a disulfide bond to Cys462 rather than forming this bond in step 5 as previously suggested. It should be added that no strain is needed for the Cys439 residue since it is protonated in the critical stage of the substrate reaction process. The modified theoretical reaction mechanism is shown in Figure 9. This modification of the mechanism does not alter the previously calculated energetics significantly (by less than 1 kcal/mol); see Figure 10.

References and Notes

(1) Voet, D.; Voet, J. G. *Biochemistry*; John Wiley and Sons: New York, 1995.
(2) Stubbe, J.; van der Donk, W. A. *Chem. Rev.* **1998**, *98*, 705−762.
(3) Sjöberg, B. M. *Structure* **1994**, *2*, 793−796. Sjöberg, B.-M. *Struct. Bonding* **1997**, *88*, 139−173.
(4) Gräslund, A.; Sahlin M. *Annu. Rev. Biophys. Biomol. Struct.* **1996**, *25*, 259−286.
(5) Reichard, P. *Science* **1993**, 260, 1773−1777.
(6) Siegbahn, P. E. M.; Blomberg, M. R. A.; Crabtree, R. H. *Theor. Chem. Acc.* **1997**, *97*, 289−300.
(7) Siegbahn, P. E. M.; Eriksson, L.; Himo, F.; Pavlov, M. *J. Phys. Chem. B* **1998**, *102*, 10622−10629.
(8) Nordlund, P.; Sjöberg, B.-M.; Eklund, H. *Nature* **1990**, *345*, 593−598.
(9) Uhlin, U.; Eklund, H. *Nature* **1994**, *370*, 533−539.
(10) Eriksson, M.; Uhlin, U.; Ramaswamy, S.; Ekberg, M.; Regnström, K.; Sjöberg, B.-M.; Eklund, H. *Structure* **1997**, *5*, 1077−1092.
(11) Stubbe, J. *Biol. Chem.* **1990**, *265*, 5330.
(12) Mao, S. S.; Holler, T. P.; Yu, G. X.; Bollinger, J. M.; Booker, S.; Johnston, M. I.; Stubbe, J. *Biochemistry* **1992**, *31*, 9733−9743.
(13) Siegbahn, P. E. M. *J. Am. Chem. Soc.* **1998**, *120*, 8417−8429.
(14) Zipse, H. *J. Am. Chem. Soc.* **1995**, *117*, 11798−11806.
(15) Stubbe, J. *Adv. Enzymol. Relat. Areas Mol. Biol.* **1990**, *63*, 349−417.
(16) Beckwith, A. L. J.; Crich, D.; Duggan, P. J.; Yao, Q. *Chem. Rev.* **1997**, *97*, 3273−3312.
(17) Lenz, R.; Giese, B. *J. Am. Chem. Soc.* **1997**, *119*, 2784−2794.
(18) Robins, M. J.; Guo, Z.; Samano, M. C.; Wnuk, S. F. *J. Am. Chem. Soc.* **1999**, *121*, 1425−1433.
(19) Persson, A. L.; Eriksson, M.; Katterle, B.; Pötsch, S.; Sahlin, M.; Sjöberg, B.-M. *J. Biol. Chem.* **1997**, *272*, 31533−31541.
(20) Persson, A. L.; Sahlin, M.; Sjöberg, B.-M. *J. Biol. Chem.* **1998**, *273*, 31016−31020.
(21) Lawrence, C. C.; Obias, H.; Stubbe, J.; Bennati, M.; Bar, G.; Griffin, R. G. *Proc. Natl. Acad. Sci. U.S.A.* **1999**, *96*, 8979−8984.
(22) Becke, A. D. *Phys. Rev.* **1988**, *A38*, 3098. Becke, A. D. *J. Chem. Phys.* **1993** *98*, 1372, 5648.
(23) Bauschlicher, C. W., Jr.; Ricca, A.; Partridge, H.; Langhoff, S. R. In *Recent Advances in Density Functional Methods*; Chong, D. P., Ed.; World Scientific Publishing Company: Singapore, 1997; Part II, p 165.
(24) Wiberg, K. A.; Keith, T. A.; Frisch, M. J.; Murcko, M. *J. Phys. Chem.* **1995**, *99*, 9072.
(25) Prabhakar, R.; Blomberg, M. R. A.; Siegbahn, P. E. M. *Theor. Chem. Acc.*, submitted.
(26) Frisch, M. J.; Trucks, G. W.; Schlegel, H. B.; Gill, P. M. W.; Johnson, B. G.; Robb, M. A.; Cheeseman, J. R.; Keith, T.; Petersson, G. A.; Montgomery, J. A.; Raghavachari, K.; Al-Laham, M. A.; Zakrzewski, V. G.; Ortiz, J. V.; Foresman, J. B.; Cioslowski, J.; Stefanov, B. B.; Nanayakkara, A.; Challacombe, M.; Peng, C. Y.; Ayala, P. Y.; Chen, W.; Wong, M. W.; Andres, J. L.; Replogle, E. S.; Gomperts, R.; Martin, R. L.; Fox, D. J.; Binkley, J. S.; Defrees, D. J.; Baker, J.; Stewart, J. P.; Head-Gordon, M.; Gonzalez, C.; Pople, J. A. *Gaussian 94*, Revision B.2; Gaussian Inc.: Pittsburgh, PA, 1995.
(27) Froese, D. J.; Humbel, S.; Svensson, M.; Morokuma, K. *J. Phys. Chem.* **1997**, *101*, 227.